

The Effect of Ice Shapes on Wind Turbine Performance

S. Barber, Y. Wang, N. Chokani and R. S. Abhari

Laboratory for Energy Conversion, ETH Zürich

ETH Zürich MLJ33, Sonneggstrasse 3, 8092 Zürich, Switzerland, barbers@ethz.ch

Abstract— Experimental studies are undertaken to examine the effects of icing on wind turbine performance. The experiments are conducted on a dynamically-scaled model in the wind turbine test facility at ETH Zürich. The central element is a water towing facility that enables full-scale non-dimensional to be more closely matched than in a wind tunnel. A novel technique is developed to yield accurate measurements of wind turbine performance. The technique incorporates the use of a torque meter with a series of systematic measurements. The results show that icing that is typical of those found at the Alpine Test Site Güttsch can reduce the power coefficient by up to 22% and the Annual Energy Production by up to 2%. Icing in the blade tip region, 95-100% blade span, has the most pronounced effect on the wind turbine’s performance. Thus it is advantageous to tailor blade heating for prevention of ice build-up to the blade’s tip region. For wind turbines in more extreme icing conditions typical of those in Bern Jura, for example, icing can result in up to 17% losses in the Annual Energy Production.

I. INTRODUCTION

A. Wind Energy in Cold Climates

WIND energy is the world’s fastest growing source of electricity production, and a key source of clean, plentiful energy for the future. In order for wind energy to fully reach its potential, the most plentiful wind farm sites must be effectively taken advantage of. As the power output of a given wind turbine is proportional to the cube of the wind velocity, a site’s capacity is highly dependent on the wind speed.

Many favourable sites for wind farms in terms of high wind speeds are located in cold, wet regions such as the northern Scandinavian coastline, the Swiss Alps, many areas of China, Northern USA and Canada. In these regions the installation of wind turbines is limited due to problems of ice formation, both on instrumentation and on the blades. Power curve predictions can be of low accuracy, and the actual performance often deviates significantly from the expected performance. This may be due to aerodynamic losses relating to ice accretion on the blades.

The improved understanding and quantification of these losses is vital for wind farm developers and investors, who must estimate accurately the expected energy production of a project in order to quantify its risks and assess its financial viability.

B. Performance and Aerodynamics

The formation of ice on airfoils is generally known to have a detrimental effect on their lift coefficient (C_L) and drag coefficient (C_D) performance. Icing on aircraft wings has been

well documented, using icing wind tunnels [1] and numerical simulation [2]. C_L was found to reduce by up to 30% and C_D was found to increase up to 50%.

The effect of icing on wind turbine blades has been less studied [3]. Power losses due to icing have been estimated to be up to 20% using 2D Computational Fluid Dynamics (CFD) and Blade Element Momentum (BEM) methods [4].

The present work involves an experimental study on the effect of icing on wind turbine performance. The work is unique in several respects. First the experiments are conducted on a dynamically-scaled model at near full-scale non-dimensional; thus the results are applicable to full-size wind turbines. Secondly the experiments involve the application of a novel power measurement method in order to accurately assess the differences in performance due to ice shapes.

The specific objective of the work is to measure the power coefficient differences caused by realistic ice shapes at a range of wind turbine tip speed ratios. The remainder of the paper discusses the experimental set-up, followed by a presentation of the results and a discussion at the end.

II. SET-UP

In this work, the performance of a three-bladed scale-model wind turbine was investigated experimentally in a water towing facility. The aluminium blades (Fig. 1) matched the S809-profile, tapered and twisted blades of the NREL Phase VI rotor from 25% to 100% span [5]. From the hub to 25% span the blade profile was modified in order to improve the structural rigidity. The effects of ice formation were investigated by attaching expected ice shapes to the blades.

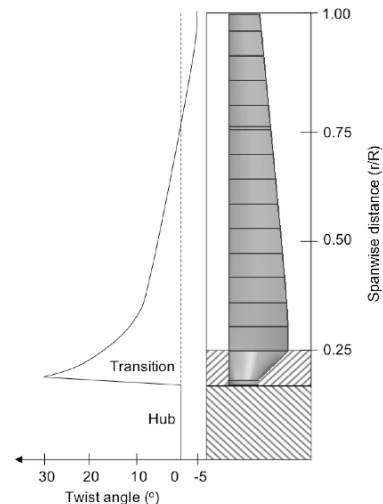


Fig. 1. The blade design.

A. Definition of Ice Shapes

The ice shapes were defined to approximate the shapes obtained from analysis of the photographs from in-situ full-scale wind turbines with icing and from results of numerical simulation of an ice accretion code. The shapes defined here are summarized in Fig. 2. The span-wise distribution refers to the span-wise extent of icing measured from the blade tip.

The photographs provided an approximate span-wise distribution of ice accumulation and served as a reference for the validation of simulated ice shapes. The 2D NASA-LEWICE ice accretion code was used to calculate the flow field around blades and provided detailed 2D ice profiles. This combined method thus enabled the reproduction of detailed 3D ice shapes.

LEWICE was used to predict 2D ice profile shapes on the blades at eight different span-wise locations. The other input parameters, as shown in Table I, were selected using conditions at the Alpine Test Site GÜtsch (Switzerland), where there is a 600 kW Enercon E40 wind turbine that regularly experiences ice formation. The wind parameters were taken as the average values over a year of data measured on the turbine and at a nearby meteorological station between the dates 01.06.2007 and 31.05.2008 (from Meteotest). In order to estimate the Liquid Water Content (LWC), simulations using the Weather Research & Forecasting model [6] were carried out by Meteotest for a typical icing event at GÜtsch. The chosen MVD (droplet diameter) was estimated based on previous LEWICE simulations [1].

TABLE I
PARAMETERS USED TO DEFINE ICING PROFILES

Turbine diameter	44 m
Turbine rotational speed	15 rpm
Wind velocity	4 m/s
Temperature	-6 °C
LWC	0.1 g/m ³
MVD	35 μm
Icing duration	10 hours

The LEWICE results for span-wise distances $r/R = 0.30$, 0.63 and 0.90 are shown in Fig. 3. The shape grows with increasing span due to the increasing rotational ($r\omega$) component of the velocity and slightly decreasing angle of attack (α).

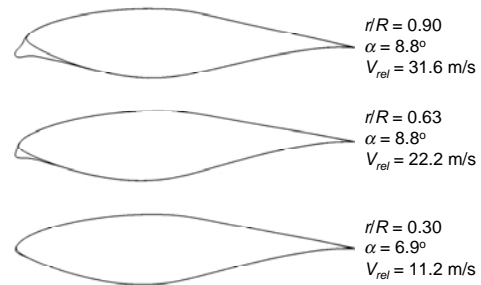


Fig. 3. Predicted ice profiles at three span-wise locations for conditions in Table I.

Test case	A	B	C	D	E	F
Profile shape						
Span-wise distribution	100 % 	25 % 	5 % 	Sawtooth 1 10% 	Sawtooth 2 5 - 20% 	100%

Fig. 2. Defined ice shapes.

The results from LEWICE were used in conjunction with photographs from the Alpine Test Site Güttsch. Approximately 11,000 photographs from a camera mounted on the nacelle of the wind turbine taken over the period between 01.06.2007 and 31.05.2008 were analyzed to establish typical span-wise distributions. It should be noted that the blades on the turbine at Güttsch are fitted with air heating systems, which are activated if the power output reaches unacceptably low values in cold temperatures. This means that the ice profiles are not extreme.

Once realistic span-wise ice distributions were established and the 2D profile shapes were predicted in LEWICE, the first five ice shapes were defined for the tests. Cases A-C represent varying length of span-wise ice formation, which result from the varying tip speed ratio conditions of the wind turbine. In each the ice shape was case linearly tapered to avoid sharp steps. Cases D and E represent the “saw-tooth” effect that was frequently observed from the photographs. This occurs when parts of the ice falls off the blade during motion. These shapes were made intentionally with sharp steps. The shapes A-E were produced in CAD using surface interpolation between the profiles predicted in LEWICE.

The final ice shape (Case F) is an extreme case that was not observed at Güttsch, but at a site where no heating system is present (e.g., Grenchenberg, Switzerland).

An example photograph from Güttsch is shown in Fig. 4 compared to the CAD drawing for Case A. The view angle is the same as the camera angle.

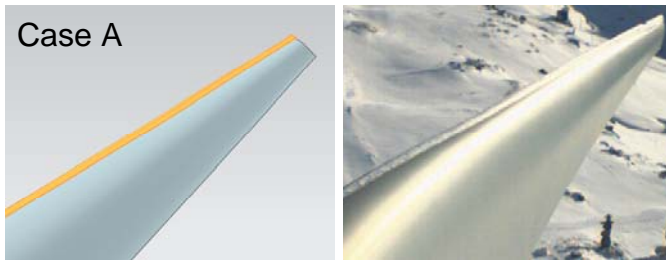


Fig. 4. Comparison of Case A with a photograph from Güttsch.

B. Experimental Set-Up

The experimental work was carried out at the sub-scale model wind turbine test facility at the Laboratory for Energy Conversion (LEC) of ETH Zürich, pictured in Fig. 5 (a). The test facility comprises a 0.3 m diameter wind turbine model that is mounted on a carriage that moves above a 40 m long, 1 m wide and 1 m deep channel of water. The velocity of the carriage can be specified to up to 3 m/s ($\pm 1\%$), as shown schematically in Fig. 4 (b). The water temperature remained at $19^\circ \pm 0.5^\circ$ throughout the measurement campaign.

The blockage ratio ($A_{rotor}/A_{channel}$) of the model is 7.1%, which is below the upper limit of 7.5% for applying corrections [7]. The wind turbine tower is inside a streamlined section, giving a Froude number for surface waves of 1.9. Thus surface and blockage effects have a negligible effect on the wind turbine performance.

The rotor blades are interchangeable and the pitch angle can be set to $\pm 2^\circ$. For the current tests the blade pitch was 0° . The rotational speed of the wind turbine is controlled by a brushless motor. The desired tip speed ratio of the wind turbine can thus be accurately specified. In this study, the turbine rotational speed was kept at 800 rpm (± 3 rpm), which avoided cavitation on the blades. The tip speed ratio was varied from 5 to 8 by varying the carriage velocity between 1.5 and 2.8 m/s.

Based on the theory of flow similarity, this facility enables the full-scale non-dimensionals to be better duplicated on a sub-scale model than in air. The Reynolds number based on mean chord at the optimal tip speed ratio of 6.0 is about 1.5×10^5 in this facility. As a comparison, the same size model in a wind tunnel would reach a Reynolds number of 3,750. The largest wind tunnel facility used for wind turbine testing (at NASA-AMES) has Reynolds numbers of the order of 1.0×10^6 whereas full-size wind turbines today even reach Reynolds numbers of the order of 1.0×10^7 . At Güttsch the Reynolds number is approximately 4.0×10^6 .

To determine the performance of the wind turbine, an in-line, contactless miniature torque-meter with measurement range 0-5 Nm (accurate to 0.1%) was installed on the shaft. Torque was converted to power by multiplying it by the rotational speed. The power of the turbine, P_{turb} , measured in the water channel, is comprised of the power required by the motor to overcome friction in the drive-train, P_{drive} , the dynamic sealing, P_{seal} , and the power absorbed by the rotor itself, P_{rotor} , which is negative for a wind turbine:

$$P_{turb} = P_{drive} + P_{seal} + P_{rotor} \quad (1)$$

Or for constant rotational velocity, ω :

$$T_{turb} = T_{drive} + T_{seal} + T_{rotor} \quad (2)$$

where T = torque (N/m^2). As depicted in Fig. 6, the measurement of T_{turb} in the water channel requires also a series of tare measurements in order to determine T_{drive} and T_{seal} .

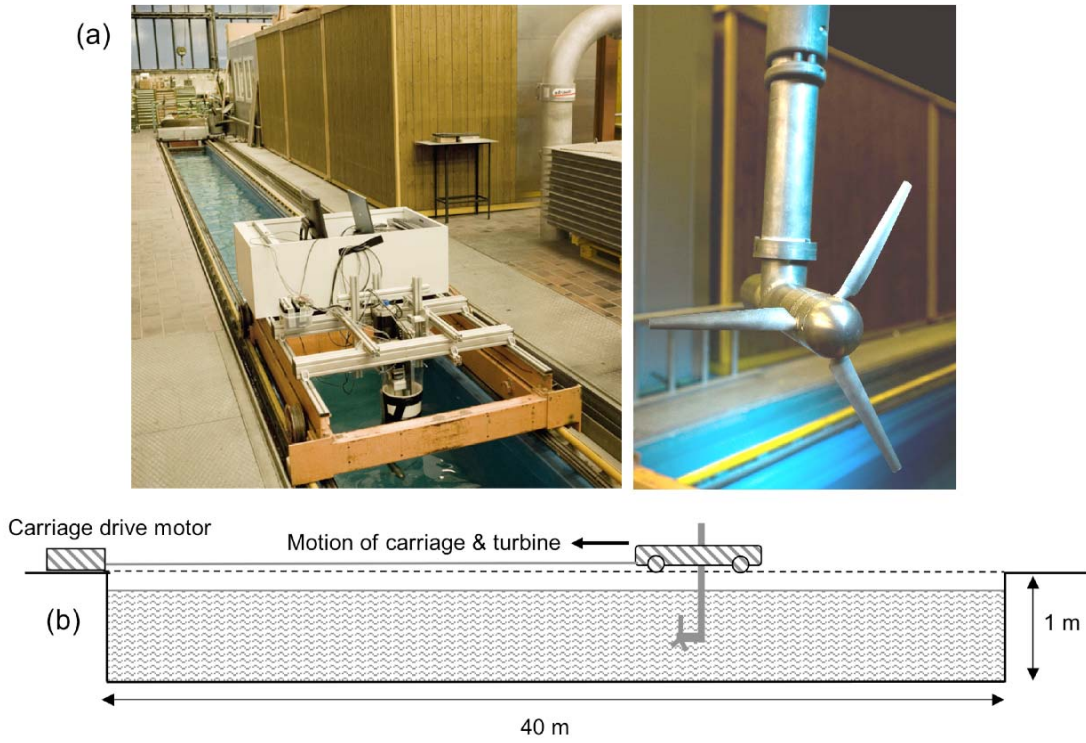


Fig. 5. LEC's sub-scale model wind turbine test facility, (a) photograph, (b) schematic diagram.

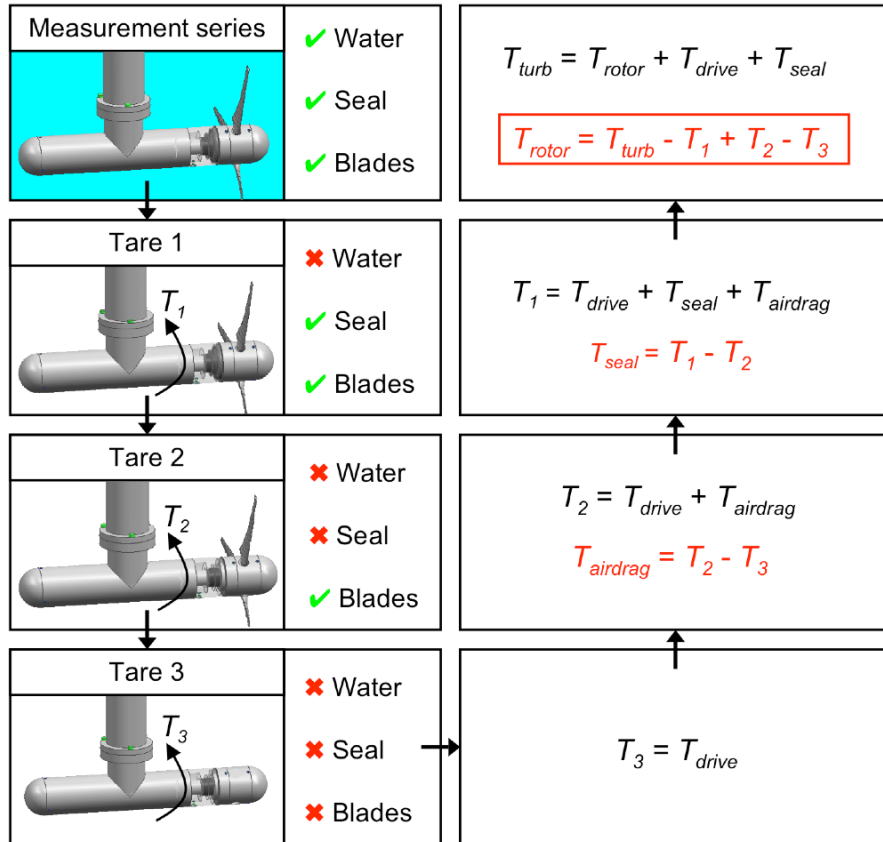


Fig. 6. Torque measurement method.

This approach assumes that the parasitic torque components due to the seal and the housing are decoupled from each other and from the torque produced by the blades. Once T_{rotor} was established for each case, the power coefficient was determined as follows:

$$C_p = \frac{T_{rotor} \omega}{\frac{1}{2} \rho V^3 A_{rotor}} \quad (3)$$

where A_{rotor} is the cross-sectional area of the rotor (m), V the carriage velocity (m/s) and ρ the fluid density (kg/m³).

The relative errors of the C_p and tip speed ratio measurements were calculated using the stated percentage errors in the translational velocity ($\pm 1\%$), rotational velocity (800 rpm ± 3 rpm), torque ($\pm 0.1\%$) and water temperature ($19^\circ \pm 0.5^\circ$). The worst case relative errors were found to be 3.0% in C_p and 1.1% in tip speed ratio.

III. RESULTS

A. Power coefficient curves

The power coefficient vs. tip speed ratio curve for the clean blades (no ice) is shown in Fig. 7. The shape is as expected for a 3-bladed wind turbine, with a peak at a tip speed ratio of approximately 6.0 – 6.5, where the power coefficient is 0.33. The rather low C_p , approximately 20% lower than full-size 3-bladed rotors [8], is expected here due to the low Reynolds number and reduced lift of the blades. Repeat measurements showed very good repeatability and a maximum variation in C_p of 1.7%, within the relative error of the experiment (section II).

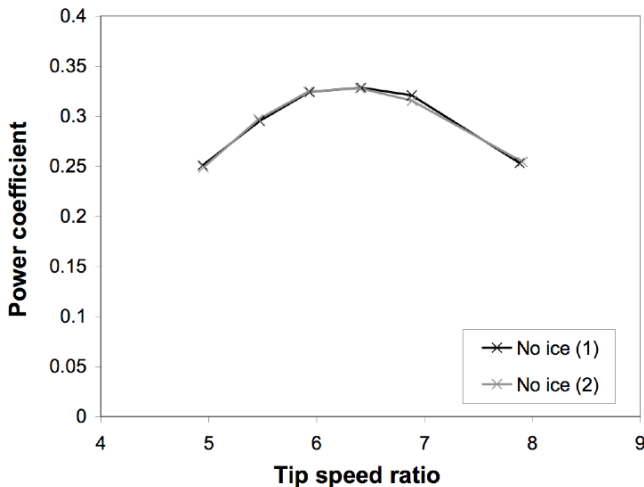


Fig. 7. Power coefficient vs. tip speed ratio graph, rotor with no ice, experiment.

The effect of icing on the wind turbine performance is shown in Fig. 8 (a) for Case A, B & C and (b) for Case D, E & F. Additionally, the relative magnitudes of C_p are examined further in Fig. 9, in which ΔC_p (the difference between C_p with ice and with no ice) for the Cases A-E for selected tip speed ratios are compared. Case F is not included for sake of clarity.

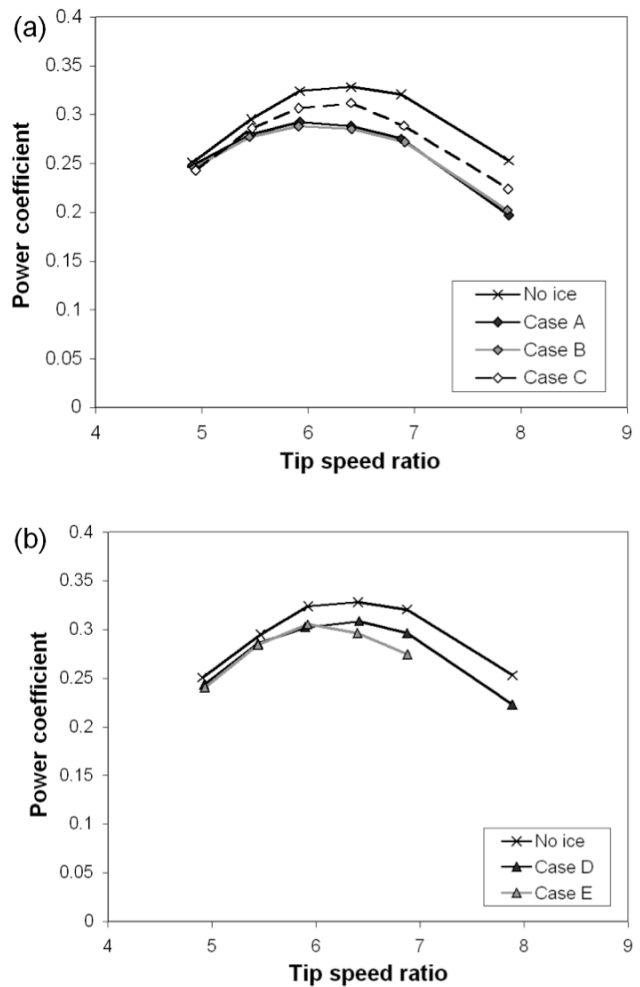


Fig. 8. Power coefficient vs. tip speed ratio graph for the rotor with ice shapes attached to blades: (a) Cases A-C compared to no ice case, (b) Cases D-F compared to no ice case.

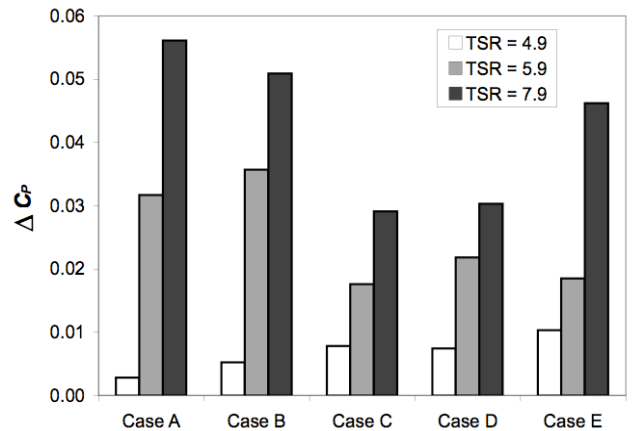


Fig. 9. ΔC_p for Cases A-E for various tip speed ratios.

It can be seen that the presence of the ice generally has a detrimental effect on the performance of the rotor. The reduction of C_p is as large as 0.06 (or 22.2%) for Cases A and B. The effect is smaller at lower tip speed ratios, and all the C_p values are within 0.01 of each other by a tip speed ratio of 4.9. This trend is expected because the losses at high tip speed ratio are mainly dictated by the aerodynamic drag of the blades, whereas the losses at low tip speed ratio are dominated by the wake angular momentum losses. The aerodynamic drag of the blades is expected to be altered due to the ice shapes, whereas the wake losses are less sensitive to blade profile and tip speed ratio. Thus the ice shapes are expected to alter C_p more significantly at higher tip speed ratios.

On examination of the uniform ice shapes (Cases A-C), it can be seen that C_p is reduced by up to 22.2% (at tip speed ratio = 7.9) for the 100%-span ice shape (Case A). The 25%-span ice shape (Case B) shows very similar behaviour, the maximum difference from Case A being 2.6% at tip speed ratio = 7.9. This suggests that only the ice in the outboard 25% of the span has a significant effect on power performance. Furthermore the reduction in performance measured for the 5% case (Case C) is approximately half that of the 25% case for the tip speed ratios close to the maximum. This means that the presence of ice on the outboard 5% of the blade has a similar impact on performance as ice on 75% to 95% of the span. This indicates a rapidly increasing effect on performance nearer the tip. Thus ice removal or prevention systems could be substantially more efficient if their effectiveness was tailored to the outboard 5% span of the blades.

Cases D and E show the effects of the two ‘‘sawtooth’’ shapes on the turbine performance. Ice Case D consists of one sharp step from the ice shape to the blade surface at 10% span. This has a very similar effect on performance as the 5% span tapered ice shape (Case C). Case E has two sharp steps from the blade to the ice shape on either side at 5% and 25% span. This ice shape has a larger influence on C_p at high tip speed ratios (C_p is 7.4% larger for Case E than for Case D at a tip speed ratio of 6.9). This again highlights the strong effect of ice that is on the outboard 5% span.

The extreme ice shape, Case F, has a major effect on the C_p . No power is generated for tip speed ratio > 6 , and the power is small for tip speed ratio < 6 .

B. Annual Energy Production

The potential effects of the ice shapes on the corresponding Annual Energy Production (AEP) of a wind turbine were estimated using the conditions at Gtsch. A continuous operation at a tip speed ratio of 5.9 (and thus the corresponding C_p measured in the above experiments) was assumed. The resulting power curves for the clean blades and for Case A are shown in Fig. 10, where the air density was taken as 1.225 kg/m^3 and the curve was cut off at the rated power of 600 kW to simulate pitch control.

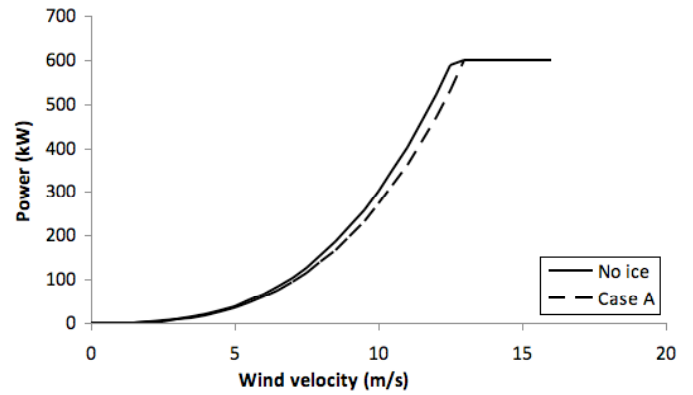


Fig. 10. Estimated power curves for the clean rotor and Case A.

The AEP was estimated using the IEC standard bins method [9], where $\varepsilon(v)$ = power curve and $f_{ref}(v)$ = measured wind speed frequency distribution over a year at the test site Gtsch:

$$AEP = \int_0^{\infty} \varepsilon(v) f_{ref}(v) dv \quad (4)$$

The resulting AEP for each case is summarized in Table II, for icing 100% of the time and for icing for only two months of the year. The two month long period was estimated as the duration of likely ice formation based on temperature data measured at Gtsch over a year together with LEWICE simulations for a range of temperatures and humidities.

TABLE II
EFFECT OF ICE ON ANNUAL ENERGY PRODUCTION

Case	12 months icing		2 months icing	
	AEP (MWh)	% loss	AEP (MWh)	% loss
Clean	121	-	121	-
Case A	109	9.8	119	1.6
Case B	108	11.0	119	1.8
Case C	115	5.4	120	0.9
Case D	113	6.7	120	1.1
Case E	114	6.9	120	0.9
Case F	0	100	101	16.7

In a separate study [10] the actual loss in AEP at Gtsch due to ice formation over a year was estimated to be approximately 1.1%, which is in good general agreement with Cases A-E. Case F, which does not occur at Gtsch, clearly has a much more devastating effect on the AEP, and may be even larger in more extreme conditions.

IV. DISCUSSION

A. Non-“extreme” ice

It was found that ice typical of that experienced by the wind turbine at GÜtsch does not cause significant losses in power and Annual Energy Production. The actual losses in power of the GÜtsch turbine are, however, much larger. This can be seen in the comparison between the manufacturer’s power curve and the measured, bin-averaged data in Fig. 11 (data obtained from Meteotest). The data is corrected for density and the velocity is taken from a meteorological station 150 m in front of the turbine. Using the standard IEC method of bins and the measured wind speed frequency distribution over a year at the test site GÜtsch, these losses were estimated to result in a loss of Annual Energy Production of 23% (from 986 MWh to 785 MWh).

Such large losses in AEP cannot be explained by the presence of ice similar to Cases A-E. Thus for the wind turbine at GÜtsch, these losses must be due to other reasons. As the wind turbine is located in highly complex terrain, effects of typical wind features in complex terrain, such as high turbulence and wind gusts, are currently being investigated further in the ETH Zürich sub-scale facility.

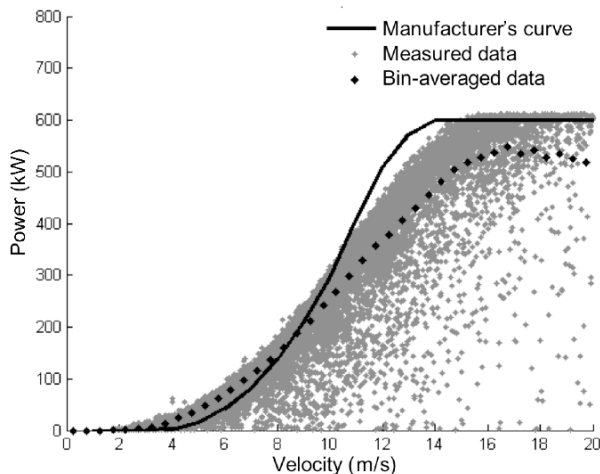


Fig. 11. Power measurements at GÜtsch (grey dots) and the bin-averaged power curve (black dots) compared to the manufacturer’s power curve (black line).

B. “Extreme” ice

It was found that “extreme” ice shapes that are large enough to cause flow separation over the entire blade can be responsible for significant power losses and reduce the AEP by an order of 20%. These ice shapes may be expected to form at altitudes in the range 800 – 1500 m such as the Bern Jura. It is thus key for wind farm developers to be able to predict the likelihood of “extreme” ice forming on the blades at planned locations.

The next steps of this study are therefore to (i) define quantitatively what is meant by “extreme” icing and (ii) combine this definition with an icing event prediction model such as the Weather Research & Forecasting model of Meteotest. Icing event prediction models are required because

the likelihood of icing events depends on a number of different factors. For example, even though the GÜtsch site is at an altitude of 2331 m, only small amounts of ice form on the blades. However, the Grenchenberg site is at a lower altitude of 1350 m but it is subject to “extreme” icing due to the particular temperature and humidity conditions there.

Ultimately this work will facilitate a tool for developers comprising a map of critical zones, where ice shapes large enough to significantly reduce the performance are likely to form.

V. CONCLUSIONS

- Ice formed at similar conditions to the Alpine Test Site GÜtsch can reduce the Annual Energy Production by up to 2%, whereas in more extreme conditions the Annual Energy Production can be reduced up to 17%.
- Ice formed at similar conditions to the Alpine Test Site GÜtsch can reduce the power coefficient by up to 0.06 (or 22.2%) at the optimal tip speed ratio; ice that builds up in more extreme conditions can reduce the power coefficient to zero.
- The effect of the ice shapes is negligible at low tip speed ratios (below 5).
- Only ice on the outboard 25% of the span has a significant impact on power performance.
- The presence of ice on the most outboard 5% of the blade has as much adverse impact on performance as the ice on 75-95% span.
- Ice shapes with a “sawtooth” span-wise distribution is no different than a uniform span-wise distribution in terms of power coefficient.
- Ice removal or prevention systems could be substantially more efficient if their effectiveness was tailored for the outboard 5% of the blade.

VI. ACKNOWLEDGMENT

The authors would like to thank the Swiss Federal Office of Energy for supporting this project. The advice & model inputs at the GÜtsch site provided by Silke Dierer (Meteotest) and the support & provision of the measurement data at GÜtsch by René Cattin (Meteotest) are greatly appreciated, as well as the technical contributions of Hans Suter, Thomas Künzle, Claudio Troller and Cornel Reshef.

VII. REFERENCES

- [1] A.P. Broeren, M.B. Bragg, and H.E. Addy, "Flowfield measurements about an airfoil with leading-edge ice shapes," *J. Aircraft*, vol. 43 (4), pp. 1226-1234, 2006.
- [2] M. Bragg, A. Broeren, H. Addy, M. Potapczuk, D. Guffond, and E. Montreuil, "Airfoil ice-accretion aerodynamics simulation," in *45th AIAA Aerospace Sciences Meeting and Exhibit*, Reno, Nevada, Jan. 2007.
- [3] N. Bose, "Icing on a small horizontal-axis wind turbine – Part 1: Glaze ice profiles," *J. Wind Eng. Ind. Aero.*, vol. 45, pp. 75-85, 1992.
- [4] M.T. Brahim, D. Chocron and I. Paraschivoiu, "Prediction of ice accretion and performance degradation of HAWT in cold climates," *AIAA-98-0026*.
- [5] P. Giguere and M.S. Selig, "Design of a tapered and twisted blade for the NREL combined experiment rotor," NREL/SR-500-26173, 1999.
- [6] W.C. Skamarock, J.B. Klemp, J. Dudhia, D.O. Gill, D.M. Barker, W. Wang and J.G. Powers, "A description of the advanced WRF version 2", National Center for Atmospheric Research, Boulder, CO, Tech. Note NCAR/TN-468+STR, Jun. 2005.
- [7] W.H. Rae, A. Pope and J.B. Barlow, *Low-Speed Wind Tunnel Testing*, 3rd ed., John Wiley & Sons, 1999.
- [8] E. Hau, *Wind Turbines*, 2nd ed., Springer Verlag, 2006.
- [9] *IEC Wind Turbine Generator Systems, Part 12: Power Performance Measurement Techniques*, IEC International Standard 61400-12, 1998.
- [10] S. Barber, N. Chokani and R.S. Abhari, "Assessment of wind turbine power performance at the alpine test site Gütsch", *poster at IWAIS 2009*, Andermatt, Switzerland, Sep. 2009.